sustainability

MDPI

Article

Microbial Synthesis of Hydroxyapatite-Nanocellulose Nanocomposites from Symbiotic Culture of Bacteria and Yeast Pellicle of Fermented Kombucha Tea

Mareeswari Paramasivan [1,2], Tiruchirapalli Subramaniam Sampath Kumar [2,*] and T. S. Chandra [1,*]

[1] Department of Biotechnology, Indian Institute of Technology Madras, Chennai 600036, India; marees26@gmail.com
[2] Medical Materials Laboratory, Department of Metallurgical and Materials Engineering, Indian Institute of Technology Madras, Chennai 600036, India
* Correspondence: tssk@iitm.ac.in (T.S.S.K.); chandrasainathan@gmail.com or chandra@iitm.ac.in (T.S.C.)

Abstract: The strong need for the utilization of industrial by-products and biowaste increases as we transition towards a circular economy. On these grounds, the present research aims to explore the applicability of the Symbiotic Culture of Bacteria and Yeast (SCOBY), a by-product of a functional beverage industry, for applications in biomedicine. Herein, hydroxyapatite (HA)-coated SCOBY nanocellulose (SN) nanocomposite (SNHA) was synthesized via a novel biomimetic approach using *Serratia marcescens* strain by adopting two different in situ approaches. Characterization studies established the presence of functional groups corresponding to pure nanocellulose and HA. Microscopic analysis revealed SN fibers of the dimensions 30–50 nm surrounded by 10–15 nm rod-shaped HA crystals. The SNHA membranes were carbonated and harbored traces of metal ions. A deposition of nano-HA crystals as high as 30–50% was achieved. Overall, the synthesized SNHA membranes reflected increased stability, low crystalline nature and an ion-substituted structure resembling the natural bone; they are thereby suited for bone tissue engineering.

Keywords: SCOBY; nanocomposite; bacterial nanocellulose; hydroxyapatite; biomimetic deposition; biomineralization; *Serratia marcescens*

Citation: Paramasivan, M.; Kumar, T.S.S.; Chandra, T.S. Microbial Synthesis of Hydroxyapatite-Nanocellulose Nanocomposites from Symbiotic Culture of Bacteria and Yeast Pellicle of Fermented Kombucha Tea. *Sustainability* **2022**, *14*, 8144. https://doi.org/10.3390/su14138144

Academic Editors: Tanmoy Roy Tusher and Mei-Fang Chien

Received: 15 June 2022
Accepted: 1 July 2022
Published: 4 July 2022

1. Introduction

Kombucha tea, a probiotic health drink, gained traction in the beverage industry as a result of its therapeutic properties. A by-product of this fermented tea, coined as SCOBY, is a thick cellulosic pellicle formed on the surface. Literature highlighted its uses as a bio-sorbent to remove heavy metal pollutants from wastewaters; as desserts or edible gums; as clothing material and in edible packaging [1]. More importantly, the properties of SCOBY, such as a high degree of purity, surface morphology, mechanical properties, water retention capacity, biocompatibility, biodegradability, water absorption, crystallinity and renewability, are comparable to that of cellulose synthesized by bacteria [1].

Bacterial cellulose and nanocellulose (BNC) are well-established for their applications in biomedicine, particularly in hard tissue regeneration procedures, owing to their pure nanofibrous structure similar to ECM, increased water-holding capacity, biocompatibility, nano-mechanical properties and classification as materials generally recognized as safe (GRAS). It is also worthy to mention that bacterial nanocellulose, unlike plant cellulose, is devoid of lignin, hemicellulose and pectin, making it eco-friendly as no harsh chemicals or treatments are required for its purification. Further, its production is extracellular thereby consuming low energy and requiring simple purification using NaOH. Additionally, BNC maintain an upper hand on a sustainable front as opposed to plant cellulose which entails deforestation, energy intensive processes, laborious biological and chemical pretreatments, disintegration and post-treatment processes [2–4]. Even from a global perspective there

prevails an inclination towards biomaterials developed from bacterial sources over vegetal sources owing to the comparative cost benefits and the purity of cellulose fibers [5].

Along these lines, hybrid inorganic–organic biocomposites of hydroxyapatite and bacterial cellulose (HA/BC) have been investigated with a view of mimicking the mineralization process of the natural bone. The basic components of the bone are mineralized nanostructures of collagen fibers, percolated and surrounded by nanocrystals of hydroxyapatite (HA) [6]. Prior research clearly depicts the clinical advantages of porous hydroxyapatite-mineralized hybrid scaffolds for bone implantation. The porous interconnected morphology of such scaffolds provides a conducive environment for osteo-integration, promoting cell adhesion, multiplication and mineralization. The mineralization subsequently supports integration between the natural bone and the scaffold, promoting faster regeneration of bone tissue [7]. BC-HA membranes displayed high osteoblast adhesion, greater nodule formation and mineralization when experimented upon for bone regeneration in calvarial defect models. No signs of cytotoxicity were visualized as well [8]. HA incorporation also enhanced mechanical strength of pure BNC membranes in addition to incurring bioactivity and osteoconductivity [9].

Among several methods for HA incorporation, biomimetic mineralization is recognized for its ability to synthesize nano-scale HA, as replication of the nanoapatite assemblage within the collagen fibers was proven to augment the ability of the scaffold for bone regeneration and repair [10]. Moreover, using biological systems renders the ability to control the structure, orientation, phase and nanoscale topography of inorganic compounds. Several organisms have been studied for their biomineralization capabilities on BNC; however, *Serratia* remains unexplored despite its potential to synthesize homogeneous HA crystals. Moreover, biomineralization using *Serratia* is quoted as a non-line-of-sight method for coating substrates with HA in pores and crevices of intricate architectures [11]. A culture of *Serratia marcescens* was deployed to synthesize nanostructured HA of uniform shape and the crystallite size thus obtained was similar to biological HA [12]. The bacterium is also known to form spherical clusters of HA nanocrystals on titanium discs. Further, Thackray, et al. used *Serratia* sp. to produce a homogeneous porous precursor bone scaffold of HA with nanocrystal dimensions. The scaffolds depicted suitable lattice structures known for promoting bone cell adhesion and microporosity known for vascularization and bone cell ingrowth [13]. The properties demonstrated as a result of planktonic mineralization by *Serratia* portrays its utilization in bone regeneration and even as a resorbable carrier for osteoblasts [11].

The present study hereby aims to provide value addition to the industrial biowaste of SCOBY as a bone grafting material by adopting simple microbial methods for the deposition of a nano form of HA. On these grounds, the outcomes of this study, including the nanocrystalline nature of synthesized HA via two novel routes, trace ion distribution on the surface of the membranes, poor crystallinity, rich carbonated groups and thermal stability, reveals the characteristics of the synthesized HA nanocomposite for its adoption in bone regeneration and tissue engineering verticals.

2. Materials and Methods

2.1. Preparation of SN

SCOBY formed via the fermentation of Kombucha tea (Figure 1, Step 1) was collected and washed several times with distilled water, followed by bleaching with 2 wt % NaOH solution in an 80 °C water bath for 30 min. Later, rinsing was carried out with distilled water and sterilization was performed by autoclaving [14,15]. In this way, pure cellulose-rich nanostructured membrane was obtained and termed as SCOBY-nanocellulose (SN).

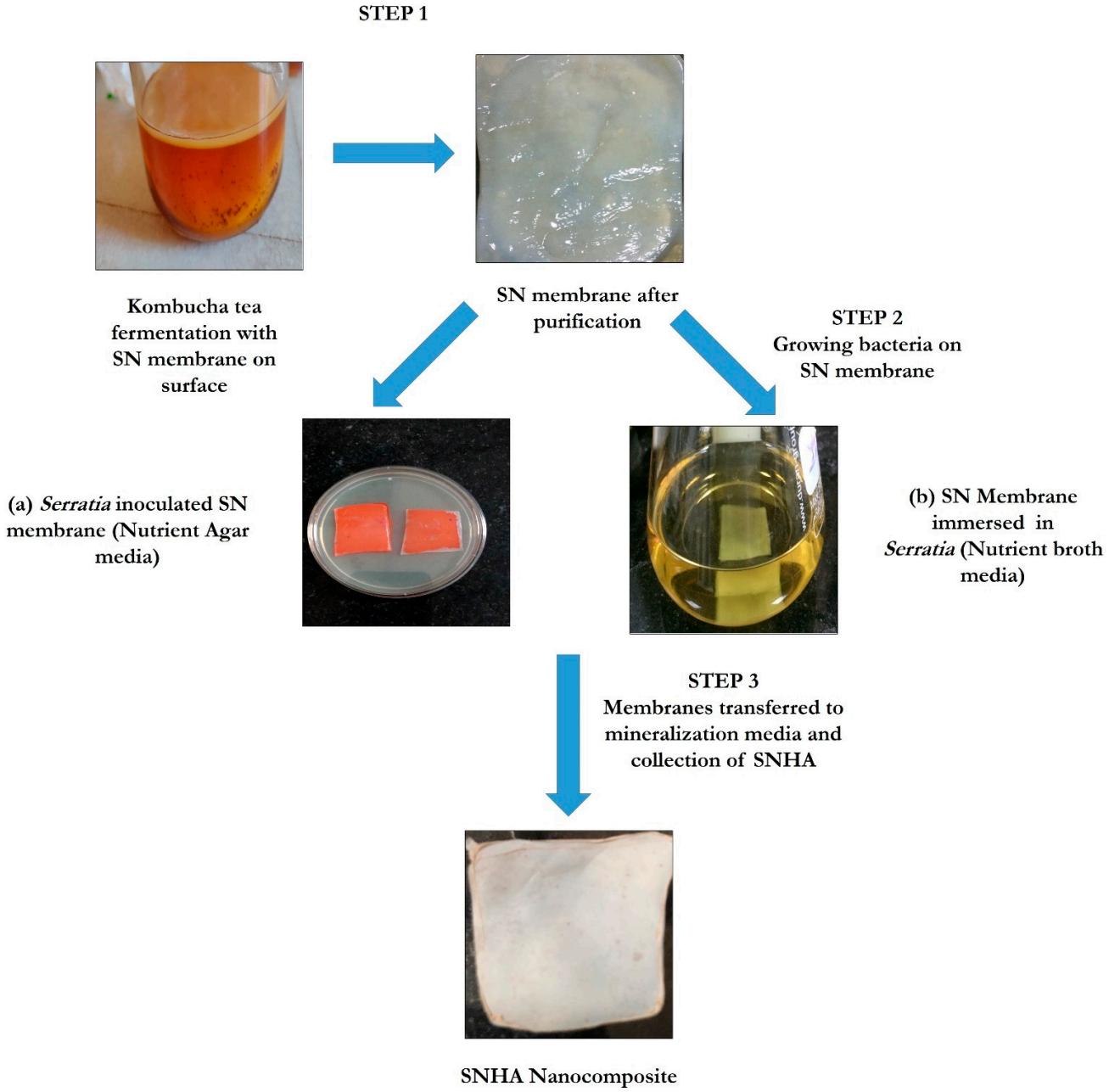

Figure 1. Schematic representation of the synthesis of SNHA nanocomposite via two methods. The white pellicle is the native nanocellulose membrane, which has turned red upon deposition of *S. marcescens* NCIM5246 on its surface in method SNHA-A, whereas in SNHA-B the nanocellulose pellicle is allowed to grow in the medium incubated at 30 °C for 15 h at 70 rpm. (Step 1: Collection of SN membrane; Step 2a: Growing *S. marcescens* NCIM5246 on SN membrane in nutrient agar plate; Step 2b: Growing S.marcescens on SN membrane in nutrient broth in a conical flask; Step 3: Transfer of the SN membrane to mineralization media and collection of the SNHA nanocomposite membranes. The optical difference in both methods can be seen from the day 1 of incubation (Figure S1)).

2.2. Preparation of SNHA Composite

The SCOBY-nanocellulose hydroxyapatite (SNHA) composite was synthesized via two different methods to achieve biomineralization. In the first method, *Serratia marcescens* (NCIM5246, NCMR Pune) was cultured on 2 × 2 cm SN membranes of wet thickness 2–3 mm on a nutrient agar plate (Figure 1, Step 2a). In the second method, the bacteria were grown along with 2 × 2 cm SN membranes of wet thickness 2–3 mm in nutrient broth

for 15 h at 70 rpm on a shaker at 30 °C. (Figure 1, Step 2b). Based on the phosphatase enzyme activity 15 h grown culture of *S. marcescens* NCIM5246 was used in both Step 2a and 2b. In Step 3, SN membranes, along with bacteria obtained from both methods, were transferred to 50 mL mineralization media consisting of 10 mM calcium chloride, 25 mM β-glycerophosphate disodium salt dihydrate, 20 mM trisodium citrate, and 25 mM tris buffer with pH adjusted to 8.5. After incubation at 30 °C (70 rpm; 10 days) these membranes were collected, dried at 40 °C and sterilized by autoclaving [12]. Thereby, two different nanocomposites were prepared; one from the agar plate, namely, SCOBY-nanocellulose-hydroxyapatite-agar plate media (SNHA-A), and one in broth termed as SCOBY-nanocellulose-hydroxyapatite-liquid broth media (SNHA-B).

2.3. Characterization Studies

The synthesized nanocomposite membranes were characterized by Scanning electron microscope (SEM) fitted with energy-dispersive X-ray spectroscopy (EDS) (FEI Quanta FEG 200, The Netherlands) after gold sputtering operated at an accelerating voltage of 10 kV. Fourier transform infrared spectroscopy was carried out (Perkin—Elmer Spectrum Two, USA) in the range of 500–4000 cm^{-1}, with a resolution of 4 cm^{-1}. Further, X-ray diffractometer (XRD) (Bruker D8 discover powder XRD, Germany) using Cukα radiation (λ = 1.54 Å) at a scanning rate of 1 step/s with a step size of 0.10 was performed. Thermo-gravimetric analysis (TGA) (Model: SDTQ600) of the sample was studied in an aluminum pan under nitrogen gas flow at a flow rate of 100 mL/min with a heating rate of 10 °C/min and a temperature range of 30–800 °C.

3. Results and Discussion

3.1. Scanning Electron Microscope Study

Kombucha fermentation yielded a three-dimensional nano-structured cellulose. These SN membranes collected from the fermented tea are known to contain yeast and bacterial cells attached to it [16]. On treatment with alkali, almost all cell debris were removed, (inset Figure 2a) and only pure cellulose fibers were witnessed. The treated SN membrane depicted a highly porous 3D nanofibrous structure (Figure 2a) with a fiber diameter of 30 to 50 nm.

SEM pictures illustrated the deposition of HA on the nanocellulosic fibers of SN (inset Figure 2b,c). Small rod-shaped HA crystals were seen surrounding the nanofibers with a well-organized 3D network on both the SNHA-A and SNHA-B membranes (Figure 2b,c). This nanofibrous network of SN, resembling a native extracellular membrane, displays a conducive platform for cell adhesion and proliferation and is greatly suited for tissue scaffold preparation [3]. The size of the HA particles was estimated to be within the range of 10 to 15 nm. Typical HA crystals were reported in an earlier study where bacterial cellulose was sequentially incubated in solutions of $CaCl_2$ and Na_2HPO_4 [17]. Such nano-HA crystals are widely known to exhibit properties of biocompatibility and bioactivity aiding applications in bone tissue engineering [18]. Moreover, a higher deposition of nano-HA crystals was visualized in SNHA-B membranes in comparison to SNHA-A membranes as a result of bacterial growth throughout the membrane. In contrast to the rosette-like crystal structure in the BNC/HA scaffolds of Sundberg, et al., the SNHA nanocrystal pattern displayed dense, rod-like crystals, similar to the BC/HA nanocomposite adsorbed with polyvinylpyrrolidone (PVP) [19,20]. Prior literature review indicates that the biomechanical features of the obtained nano-sized HA closely mimic natural bone composition in addition to demonstrating an accelerated response to stimuli, increased delivery rates and controlled release of bioactives. These traits consequently improve osteo-regenerative properties. The nanocrystalline structure was also highlighted for its higher surface to volume ratio which enhances sinterability and densification for effective fracture toughness and mechanical properties [21].

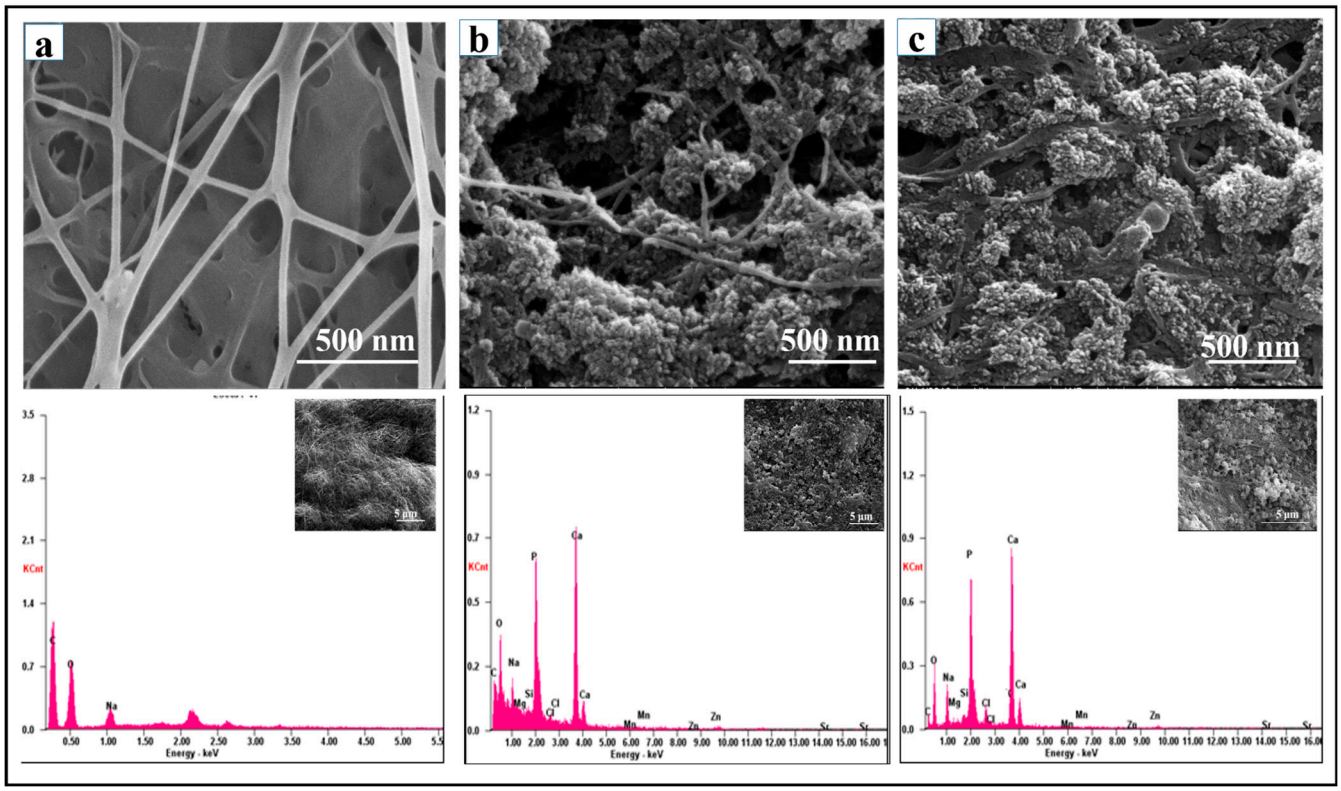

Figure 2. SEM micrographs and their corresponding EDS images of (**a**) alkali-treated SN (**b**) SNHA-A nanocomposite (**c**) SNHA-B nanocomposite and corresponding low-resolution images are shown insets.

The EDS spectrum of the nanocomposite detected traces of mineral ions such as strontium, magnesium, zinc and sodium on the SNHA membranes. The prevalence of ions is a direct result of alkaline phosphatase (ALP) activity of *S. marcescens* NCIM5246. ALP is a vital enzyme involved in the mineral formation of the natural bone [22]. The enzyme activity ideally triggered the release of inorganic phosphate ions in the media, which further reacted with calcium ions to form hydroxyapatite crystals [23]. When live cells of *S. marcescens* NCIM5246 are challenged with calcium chloride and glycerol-2-phosphate, extracellular crystals of calcium-deficient HA are produced (Figure 2b). The lipopolysaccharide (LPS) then acts as nucleation sites for Ca^{2+} ions to bond with PO_4^- ions. Meanwhile, the enzyme catalyzes the cleavage of organic phosphate and releases HPO_4^{2-}. This in turn reacts with percolated Ca^{2+} on LPS to form HA. It was also reported that, followed by small amount of organic phosphate, HA can be synthesized from inorganic phosphates present in wastewaters as well, which favors sustainable manufacturing processes [24].

More specifically, each of the ions usually termed foreign ions carry out specific functions in the remodeling and regeneration of bone. The imbalance of charges in calcium-deficient HA is fulfilled by the incorporation of ions including Mg^{2+}, K^+, Na^+, Sr^{2+}, CO_3^{2-} and SiO_4^{4-}. Such a feat results in a poor crystalline phase, higher specific area, better solubility and bioavailability [25]. The poor crystallinity is clearly revealed by the XRD results below (Figure 3).

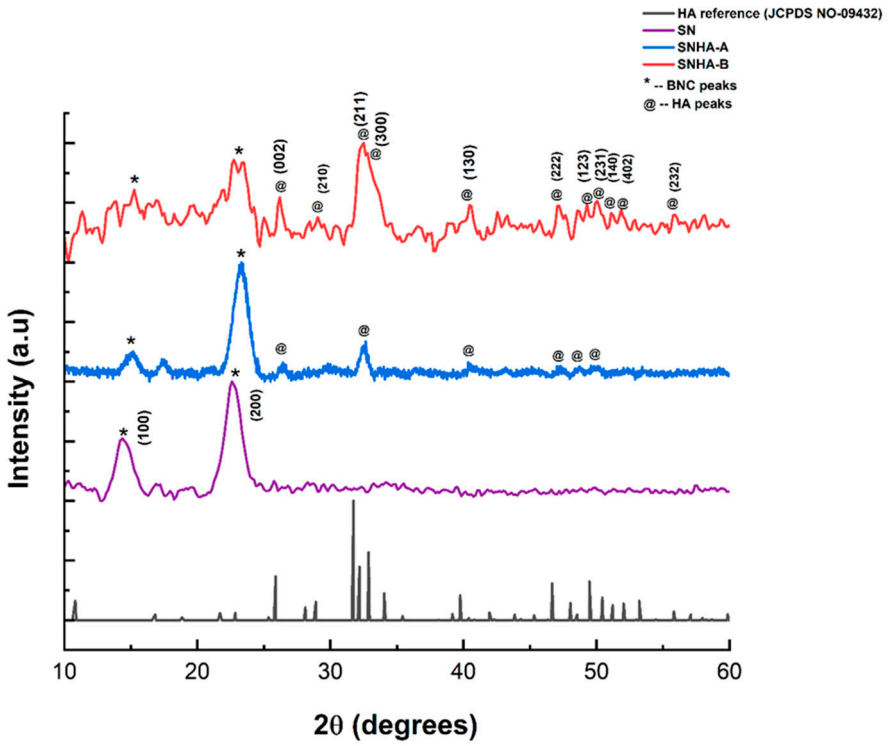

Figure 3. XRD spectra of the standard HA (JCPDS NO 09432), SN, SNHA-A and SNHA-B nanocomposites.

Taking into account the aforementioned mechanisms, the biomineralization process of *S. marcescens* NCIM5246 clearly mimics that of the natural bone wherein hydroxyapatite mineralizes on the matrix via calcium and phosphate ion deposition from blood plasma [7]. SNHA membranes bearing ion-substituted HA is thereby advantageous in bone tissue engineering owing to its matrix resemblance to that of natural bone components [26].

3.2. FTIR Characterization

The ATR-FTIR spectra of SN were found to be identical to pure cellulose (Figure 4) owing to presence of hydroxyl groups and hydrogen bonds (3200–3500 cm^{-1}). Furthermore, the absorption intensities at 1155 cm^{-1} and 1045 cm^{-1} corresponded to the C-O-C asymmetric stretching and C-O bond stretching modes of SN, respectively [27,28]. In both the SNHA-A and SNHA-B membranes, as opposed to SN, the stretching vibrations of hydroxyl groups is seen as strong broad adsorption bands indicating their interactions with HA. The crosslinking of Ca^{2+} from nano-HA with -OH groups or through hydrogen bonding was shown to aid the interfacial behavior and strength of biocomposites [29]. Besides, both the spectra revealed functional groups corresponding to HA at 1020, 600 and 559 cm^{-1} (Figure 4). Peaks obtained at 1020 and 963 cm^{-1} portrayed the stretching mode of the PO_4^{3-} vibration of pure HA, while intensities at 600 and 559 cm^{-1} were attributed to bending O-P-O bonds of phosphate groups. Notably, the characteristic P-O bonds in HA (1020 cm^{-1}) was found to overlap with the C-O-C groups of SN [6] evincing the deposition of HA on SN. More importantly, two functional groups of CO_3^{2-} and HPO_4^{2-} (1422 and 873 cm^{-1}) were seen as present in biological HA [12]. This indicates the presence of carbonate ions in both the SNHA-A and SNHA-B membranes. Thereby, the HA deposited on SN can be identified as carbonate-containing HA [19]. Results showed that carbonate-containing HA crystals were deposited on the 3D fibrous network of both SNHA membranes and they bear functional groups similar to that of biological HA. Such illustrations are consistent with the composition of the natural bone [30]. It is also vital to indicate that similar to prior results, the 963 cm^{-1} peak was found to lay on the shoulder of 1029 cm^{-1} as opposed to a sharp band in the standard HA spectra. This reveals the poorly crystalline nature of HA which is in agreement with XRD results given below [31].

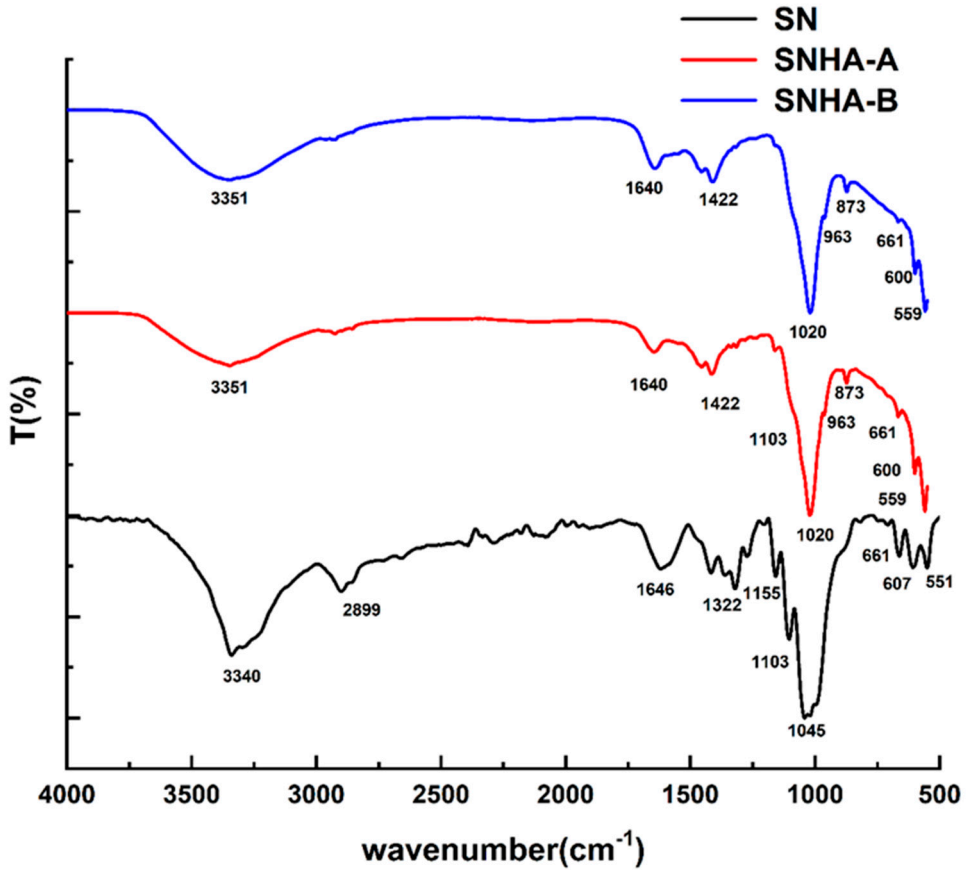

Figure 4. ATR-FTIR spectra of the SN, SNHA-A and SNHA-B nanocomposites.

3.3. X-ray Diffraction Study

The XRD pattern of SN is shown in Figure 3. Peaks located at 14.2° and 22.4° were assigned to (100) Iα,(110) Iβ, (010) Iβ, (110) Iα and (002) Iβ crystallographic planes of cellulose I, comprising of Iα and Iβ allomorphs [17,27]. Broad diffraction peaks similar to bacterial cellulose reported by Grande, et al. were observed [32]. The crystallinity index (CI) was calculated by the equation.

$$CI = [(I_{200}) - (I_{am})/I_{200})] \times 100$$

where I_{200} is the intensity of (200) peak at 2θ = 22.4° and I_{am} is the intensity of diffraction peak at 2θ = 18° [33]. The crystallinity index of the SN membrane was around 90% which was higher than that of the Kombucha synthesized bacterial cellulose produced by Zhu, et al. [34]. The XRD pattern of the SNHA-A and SNHA-B samples confirmed the presence of HA peaks at 25.8, 31.8, 40° in accordance with the HA reference pattern (JCPDS NO-09432) [35] (Figure 3). Further, a decrease in the intensity of cellulose peaks can be attributed to the deposition of HA [17]. The XRD data were in alignment with reports by Grande, et al. wherein HA particles were introduced in the culture medium during the formation of cellulose nanofibrils [32]. Moreover, in both the sample preparation methods, characteristic peaks of HA were broad; which displayed the low crystallinity of HA. Poorly crystalline HA has been reported previously [19,31,36,37]. This very low crystalline nature is essential to enhance the in vivo resorbability rates for biomedical scaffolds [38]. Similar reduced crystallinity along with increased thermal stability was reported earlier in a BNC/HA composite via cellulose nanocrystal-assisted dispersibility method [39], while Asha, et al. highlighted the increase in mineralization with an increase in incubation days via a decrease in the crystallinity index. Such mineralization of hydroxyapatite on nanocellulose membranes promotes the integration between the membrane and bone, thereby accelerating the bone regeneration process [7].

3.4. Thermogravimetric Analysis

Thermogravimetric (TGA) studies were carried out to estimate the thermal stability of the prepared nanocomposites (Figure 5). The decomposition of SN was found to be around 320–350 °C (Figure 5) which was in agreement with the range reported by Dima, et al. [27]. In similar fashion, both the SNHA-A and SNHA-B membranes decomposed around 320–350 °C. However, both displayed weight loss which could be attributed to the dehydroxylation and decomposition of organic molecules [17]. There was no weight loss after 650 °C, indicating that all the organic components were decomposed. Yet only the mineral phase of the apatite remained stable even at higher temperatures. In SNHA-A, the mineral phase constituted around 35% of the total weight, whereas in SNHA-B the mineral phase was around 50% of the total weight of the nanocomposite. It was clearly understood that the sample deposition of HA was higher in SNHA-B compared to SNHA-A, likely influenced by their preparation protocols. Carbonaceous residue of around 20% was observed in SN; 55% in SNHA-A and 70% in SNHA-B, from which the HA deposition on SN membranes was around 35 and 50%, respectively. Similar thermogravimetric results were discussed earlier by Zhang, et al., wherein HA-coated bacterial nanocellulose exhibited a residue of around 50% at 700 degrees after immersion in simulated body fluid [40], whereas Grande, et al. reported a 23.7% mineral phase of the synthesized bacterial cellulose- and calcium-deficient hydroxyapatite nanocomposite [32]. Further, a 25% residue (indicative of a lower 7% HA content) was revealed in an HA-coated bacterial cellulose scaffold prepared using Gluconacetobacter hansenii [41]. The higher abundance of HA distribution in SN membranes coupled with stability at increased temperatures advocates its suitability in bone graft repair.

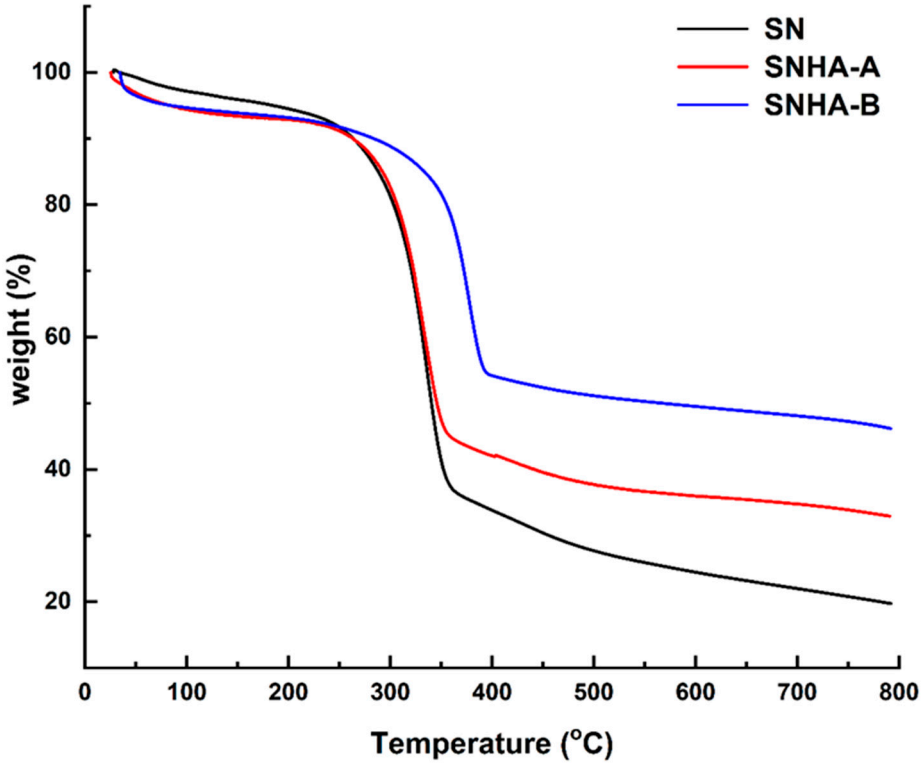

Figure 5. TGA spectra of the SN, SNHA-A, SNHA-B nanocomposites.

3.5. Deposition of HA on SN Membrane by S. marcescens NCIM5246

The culturing of *S. marcescens* NCIM5246 *a* has produced extracellular crystals of HA on the nanocellulose membranes via the enzymatic cleavage of β-glycerophosphate in the presence of calcium chloride (Figure 1; steps 2 to 3). The non-pathogenic Gram-negative bacterium is known to over-produce the phosphatase enzyme which results in HA deposition. In the agar plate technique (SNHA-A), the growth of *S. marcescens* NCIM5246

was confined precisely to the membrane, indicative of bacterial entrapment onto the surface of SN alone (Figure 1: Step 2a). Meanwhile, in the second method (SNHA-B), utilizing a liquid medium, the bacterial growth and subsequent deposition of HA extended to the interior pores of the membrane (Figure 1: Step 2b). Consequently, a higher surface deposition of HA on SN membranes was visualized. This can be attributed to the free-flowing access of *S. marcescens* NCIM5246 to react with the SN membrane, as opposed to the agar plate technique. The SNHA-B nanocomposite synthesis route is thus more advantageous in terms of higher thermal stability and denser deposition of HA nanocrystals spread throughout the SN membrane. The infiltration of nanocompartments of SN by HA was achieved successfully by adopting biomimetic methods. This indicates that the SN membranes acted as insoluble collagen fibrils, as in the case of natural bone, by providing conducive nanocompartments for mineral deposition [42].

Upon comparison with similar BNC/HA nanocomposites, varying results have been obtained as shown in Table 1.

Table 1. BNC/HA nanocomposites and their findings compared to the present research.

S. No	Nano Composite Studied	Technique Used	Inducers	Description of Material	Characteristic Application	References
1.	BNC/HA	Calcium phosphate mineralization	Paraffin particles as porogens	Rosette-like crystal structure HA; stiffer biomaterial	Improves osteoconductivity	[20]
2.	OBC-HA-G	Immersing BC in cycles of $CaCl_2$ and Na_2HPO_4	Oxidization of BC with immersion in gelatin	Poor crystallinity; a greater load-bearing capacity and mechanical strength	Promote adhesion and proliferation of the bone cells; complexation of Ca^{2+} in the composites	[36]
3.	HAp/BNC	7 day immersion in 1.5 × SBF	$CaCl_2$ immersion; PVP	Spherical rod-like carbonate-apatite crystals; low crystallinity	Facilitate cell adhesion	[19]
4.	HA/BC	1.5 × SBF solution at 37 °C for 14 days	Chemical pretreatment with $CaCl_2$	Dense homogeneous particles of calcium-deficient HA even beneath the surface; poorly crystalline HA	Bone tissue engineering	[37]
5.	HAp/BC	1.5 × SBF solution at 37 °C for 7 or 14 days	$CaCl_2$ and phosphorylation	Poor crystallinity; HAp crystals with needle-like shape	Control of in vivo resorbability rates; Biodegradability	[31]
6.	BC/HA	Alternating incubation cycles with calcium and phosphate solutions	-	Surface deposition of 50% of HA in the BC (weight calculated by comparison with control cellulose weight)	Osteoblast proliferation; Greater nodule formation and mineralization	[15]
7.	HA-coated BC	5 × SBF solution	Irradiated at 300 kGy by an electron beam accelerator	7% HA content (TGA); HA spherical only on the surface of BC	No inflammatory reactions	[41]
8.	SNHA-A and SNHA-B	*S. marcescens* NCIM5246 in biomineralization media	-	Poor crystallinity; 50% HA desposition even inside pores of SN; thermal stability	High resemblance to bone composition and mechanism	Present study

Table 1 clearly depicts the novelty of the adopted method to utilize live *S. marcescens* NCIM5246 for HA deposition with the amount of deposition as high as 50%. Despite the clear resemblance to natural bone parameters as evinced by characterization studies and distribution densities of HA, the present study only provides a preliminary assessment of the potential of SNHA. Several factors need to be examined prior to scaling up research. Previously, Silva, et al. evaluated the biological behavior of synthetic hydroxyapatite when implanted in dental cavities and covered with nanocellulose. It was found that nanocellulose associated to the HA promoted faster bone regeneration in comparison with the control. However, there were certain limitations, such as the presence of an infection caused by periodontal disease and periapical lesions. Further, even a study on mongrel dogs showed negligible improvements compared to the control [29]. Real-time experiments would better predict the need for any modifications that could improve the functionality of SNHA. Nevertheless, compared to present researched materials (Table 1) in terms of sustainability, characteristic traits, homogenous 3D nanofibrous structure morphology and amount of HA deposition, SNHA synthesis via *S. marcescens* NCIM5246 holds immense potential for bone tissue engineering applications.

4. Conclusions

The capacity of a nanocellulosic by-product from the Kombucha tea industry as a potential biomedical material was explored. The use of live *S. marcescens* NCIM5246 cultures for depositing HA on SN was reported for the first time, adopting two different growth methodologies. HA deposition as high as 50% was witnessed via culturing in liquid broth medium. Such live bacterial deposition methods enable better control of the distribution and density of HA in SNHA nanocomposites. Essentially, the highly porous nanostructure incorporated with nano-HA crystals, significant trace ion distribution, stability at high temperatures and low crystalline nature of the SNHA membrane indicates its applicability in bone grafting. Future research aims to establish the biocompatibility, biodegradability, mechanical and biochemical properties of SNHA via in vivo and in vitro studies. Additionally, the economic feasibility of production and sustainable manufacturing processes shall be estimated to aid commercialization prospects.

5. Patents

An Indian patent has been filed based on the work completed above.

Supplementary Materials: The following supporting information can be downloaded at: https://www.mdpi.com/article/10.3390/su14138144/s1. Figure S1: SEM micrographs of cross-sections of BNC-HA nanocomposite (a) SNHA-A nanocomposite (b) SNHA-B nanocomposite. Figure S2: SEM and EDS spectra of HA nanoparticles. Figure S3: TEM micrograph of HA nanoparticles with SAED pattern.

Author Contributions: M.P.: Conceptualization, methodology, investigation, formal analysis, validation, visualization, writing—original draft, writing—review and editing. T.S.S.K.: Conceptualization, methodology, formal analysis, supervision, writing—review and editing. T.S.C.: Conceptualization, methodology, formal analysis, supervision, funding acquisition, writing—review and editing. All authors have read and agreed to the published version of the manuscript.

Funding: This research did not receive any specific grant from funding agencies in the public, commercial, or not for profit sectors.

Institutional Review Board Statement: Not applicable.

Informed Consent Statement: Not applicable.

Data Availability Statement: Not applicable.

Acknowledgments: Author Mareeswari Paramasivan is thankful to MHRD, Government of India for the HTRA fellowship to support this research. The authors thank the Department of Chemical Engineering, Sophisticated Analytical Instrument Facility (SAIF), Central XRD-IIT Madras for the analytical support. The authors gratefully acknowledge support from IC&SR IIT Madras, under the Innovative Project Scheme.

Conflicts of Interest: The authors declare that they have no conflict of interest.

References

1. Coelho, R.M.D.; de Almeida, A.L.; Amaral, R.Q.G.D.; da Mota, R.N.; de Sousa, P.H.M. Kombucha: Review. *Int. J. Gastron. Food Sci.* **2020**, *22*, 100272. [CrossRef]
2. Kumar, A.; Han, S.-S. Efficacy of Bacterial Nanocellulose in Hard Tissue Regeneration: A Review. *Materials* **2021**, *14*, 4777. [CrossRef]
3. Halib, N.; Ahmad, I.; Grassi, M.; Grassi, G. The remarkable three-dimensional network structure of bacterial cellulose for tissue engineering applications. *Int. J. Pharm.* **2019**, *566*, 631–640. [CrossRef]
4. Knöller, A.; Widenmeyer, M.; Bill, J.; Burghard, Z. Fast-Growing Bacterial Cellulose with Outstanding Mechanical Properties via Cross-Linking by Multivalent Ions. *Materials* **2020**, *13*, 2838. [CrossRef]
5. Swingler, S.; Gupta, A.; Gibson, H.; Kowalczuk, M.; Heaselgrave, W.; Radecka, I. Recent Advances and Applications of Bacterial Cellulose in Biomedicine. *Polymers* **2021**, *13*, 412. [CrossRef]
6. Qi, Y.; Cheng, Z.; Ye, Z.; Zhu, H.; Aparicio, C. Bioinspired Mineralization with Hydroxyapatite and Hierarchical Naturally Aligned Nanofibrillar Cellulose. *ACS Appl. Mater. Interfaces* **2019**, *11*, 27598–27604. [CrossRef]
7. Asha, S.; Ananth, A.N.; Jose, S.P.; Rajan, M.A.J. Reduced graphene oxide aerogel networks with soft interfacial template for applications in bone tissue regeneration. *Appl. Nanosci.* **2018**, *8*, 395–405. [CrossRef]
8. Pigossi, S.C.; De Oliveira, G.J.P.L.; Finoti, L.S.; Nepomuceno, R.; Spolidorio, L.C.; Rossa, C.; Ribeiro, S.J.L.; Saska, S.; Scarel-Caminaga, R.M. Bacterial cellulose-hydroxyapatite composites with osteogenic growth peptide (OGP) or pentapeptide OGP on bone regeneration in critical-size calvarial defect model. *J. Biomed. Mater. Res. Part A* **2015**, *103*, 3397–3406. [CrossRef]
9. Jiang, P.; Ran, J.; Yan, P.; Zheng, L.; Shen, X.; Tong, H. Rational design of a high-strength bone scaffold platform based on *in situ* hybridization of bacterial cellulose/nano-hydroxyapatite framework and silk fibroin reinforcing phase. *J. Biomater. Sci. Polym. Ed.* **2017**, *29*, 107–124. [CrossRef]
10. Li, Y.; Chen, X.; Fok, A.; Rodriguez-Cabello, J.C.; Aparicio, C. Biomimetic Mineralization of Recombinamer-Based Hydrogels toward Controlled Morphologies and High Mineral Density. *ACS Appl. Mater. Interfaces* **2015**, *7*, 25784–25792. [CrossRef]
11. Lsammons, R.; Thackray, A.C.; Ledo, H.M.; Marquis, P.M.; Jones, I.P.; Yong, P.; Macaskie, L.E. Characterisation and sintering of nanophase hydroxyapatite synthesised by a species of Serratia. *J. Phys. Conf. Ser.* **2007**, *93*, 012048. [CrossRef]
12. Mostaghaci, B.; Fathi, M.H.; Zeinoddin, M.S.; Zad, S.S. Bacterial synthesis of nanostructured hydroxyapatite using Serratia marcescens PTCC 1187. *Int. J. Nanotechnol.* **2009**, *6*, 1015. [CrossRef]
13. Thackray, A.C.; Sammons, R.L.; Macaskie, L.E.; Yong, P.; Lugg, H.; Marquis, P.M. Bacterial biosynthesis of a calcium phosphate bone-substitute material. *J. Mater. Sci. Mater. Electron.* **2004**, *15*, 403–406. [CrossRef]
14. Gea, S.; Reynolds, C.T.; Roohpour, N.; Wirjosentono, B.; Soykeabkaew, N.; Bilotti, E.; Peijs, T. Investigation into the structural, morphological, mechanical and thermal behaviour of bacterial cellulose after a two-step purification process. *Bioresour. Technol.* **2011**, *102*, 9105–9110. [CrossRef]
15. Tazi, N.; Zhang, Z.; Messaddeq, Y.; Almeida-Lopes, L.; Zanardi, L.M.; Levinson, D.; Rouabhia, M. Hydroxyapatite bioactivated bacterial cellulose promotes osteoblast growth and the formation of bone nodules. *AMB Express* **2012**, *2*, 61. [CrossRef]
16. Jayabalan, R.; Malbaša, R.V.; Sathishkumar, M. Kombucha Tea: Metabolites. In *Fungal Metabolites*; Springer: Cham, Switzerland, 2017; pp. 965–978. [CrossRef]
17. Saska, S.; Barud, H.S.; Gaspar, A.M.M.; Marchetto, R.; Ribeiro, S.J.L.; Messaddeq, Y. Bacterial Cellulose-Hydroxyapatite Nanocomposites for Bone Regeneration. *Int. J. Biomater.* **2011**, *2011*, 175362. [CrossRef]
18. Lett, J.A.; Sagadevan, S.; Fatimah, I.; Hoque, E.; Lokanathan, Y.; Léonard, E.; Alshahateet, S.F.; Schirhagl, R.; Oh, W.C. Recent advances in natural polymer-based hydroxyapatite scaffolds: Properties and applications. *Eur. Polym. J.* **2021**, *148*, 110360. [CrossRef]
19. Yin, N.; Chen, S.-Y.; Ouyang, Y.; Tang, L.; Yang, J.-X.; Wang, H.-P. Biomimetic mineralization synthesis of hydroxyapatite bacterial cellulose nanocomposites. *Prog. Nat. Sci.* **2011**, *21*, 472–477. [CrossRef]
20. Sundberg, J.; Götherström, C.; Gatenholm, P. Biosynthesis and in vitro evaluation of macroporous mineralized bacterial nanocellulose scaffolds for bone tissue engineering. *Bio-Med. Mater. Eng.* **2015**, *25*, 39–52. [CrossRef]
21. Zhao, R.; Yang, R.; Cooper, P.; Khurshid, Z.; Shavandi, A.; Ratnayake, J. Bone Grafts and Substitutes in Dentistry: A Review of Current Trends and Developments. *Molecules* **2021**, *26*, 3007. [CrossRef]
22. De Jonge, L.T.; Leeuwenburgh, S.C.G.; Beucken, J.J.J.P.V.D.; Wolke, J.G.C.; Jansen, J.A. Electrosprayed Enzyme Coatings as Bioinspired Alternatives to Bioceramic Coatings for Orthopedic and Oral Implants. *Adv. Funct. Mater.* **2009**, *19*, 755–762. [CrossRef]

23. Pompei, R.; Ingianni, A.; Foddis, G.; Di Pietro, G.; Satta, G. Patterns of Phosphatase Activity among Enterobacterial Species. *Int. J. Syst. Bacteriol.* **1993**, *43*, 174–178. [CrossRef]
24. Sammons, R.; Wang, A.; Mikheenko, I.; Handley-Sidhu, S.; Macaskie, L.E. *Bacterially Derived Nanomaterials and Enzyme-Driven Lipid-Associated Metallic Particle Catalyst Formation*, 1st ed.; Elsevier Inc.: Amsterdam, The Netherlands, 2013.
25. Sprio, S.; Sandri, M.; Panseri, S.; Iafisco, M.; Ruffini, A.; Minardi, S.; Tampieri, A. *Bone Substitutes Based on Biomineralization*; Woodhead Publishing Limited: Sawston, UK, 2014.
26. Habraken, W.; Habibovic, P.; Epple, M.; Bohner, M. Calcium phosphates in biomedical applications: Materials for the future? *Mater. Today* **2015**, *19*, 69–87. [CrossRef]
27. Dima, S.-O.; Panaitescu, D.-M.; Orban, C.; Ghiurea, M.; Doncea, S.-M.; Fierascu, R.C.; Nistor, C.L.; Alexandrescu, E.; Nicolae, C.-A.; Trică, B.; et al. Bacterial Nanocellulose from Side-Streams of Kombucha Beverages Production: Preparation and Physical-Chemical Properties. *Polymers* **2017**, *9*, 374. [CrossRef]
28. Grube, M.; Shvirksts, K.; Denina, I.; Ruklisa, M.; Semjonovs, P. Fourier-transform infrared spectroscopic analyses of cellulose from different bacterial cultivations using microspectroscopy and a high-throughput screening device. *Vib. Spectrosc.* **2016**, *84*, 53–57. [CrossRef]
29. Thakur, V.K. *Nanocellulose Polymer Nanocomposites*; Wiley: Hoboken, NJ, USA, 2014.
30. Verma, A.H.; Kumar, T.S.S.; Madhumathi, K.; Rubaiya, Y.; Ramalingan, M.; Doble, M. Curcumin Releasing Eggshell Derived Carbonated Apatite Nanocarriers for Combined Anti-Cancer, Anti-Inflammatory and Bone Regenerative Therapy. *J. Nanosci. Nanotechnol.* **2019**, *19*, 6872–6880. [CrossRef]
31. Wan, Y.; Huang, Y.; Yuan, C.; Raman, S.; Zhu, Y.; Jiang, H.; He, F.; Gao, C. Biomimetic synthesis of hydroxyapatite/bacterial cellulose nanocomposites for biomedical applications. *Mater. Sci. Eng. C* **2007**, *27*, 855–864. [CrossRef]
32. Grande, C.J.; Torres, F.G.; Gomez, C.; Bañó, C. Nanocomposites of bacterial cellulose/hydroxyapatite for biomedical applications. *Acta Biomater.* **2009**, *5*, 1605–1615. [CrossRef]
33. Segal, L.; Creely, J.J.; Martin, A.E., Jr.; Conrad, C.M. An Empirical Method for Estimating the Degree of Crystallinity of Native Cellulose Using the X-Ray Diffractometer. *Text. Res. J.* **1959**, *29*, 786–794. [CrossRef]
34. Zhu, C.; Li, F.; Zhou, X.; Lin, L.; Zhang, T. Kombucha-synthesized bacterial cellulose: Preparation, characterization, and biocompatibility evaluation. *J. Biomed. Mater. Res. Part A* **2013**, *102*, 1548–1557. [CrossRef]
35. Rameshbabu, N.; Rao, K.P.; Kumar, T.S.S. Acclerated microwave processing of nanocrystalline hydroxyapatite. *J. Mater. Sci.* **2005**, *40*, 6319–6323. [CrossRef]
36. Yang, M.; Zhen, W.; Chen, H.; Shan, Z. Biomimetic design of oxidized bacterial cellulose-gelatin-hydroxyapatite nanocomposites. *J. Bionic Eng.* **2016**, *13*, 631–640. [CrossRef]
37. Hong, L.; Wang, Y.; Jia, S.; Huang, Y.; Gao, C.; Wan, Y. Hydroxyapatite/bacterial cellulose composites synthesized via a biomimetic route. *Mater. Lett.* **2006**, *60*, 1710–1713. [CrossRef]
38. Zimmermann, K.A.; LeBlanc, J.M.; Sheets, K.T.; Fox, R.W.; Gatenholm, P. Biomimetic design of a bacterial cellulose/hydroxyapatite nanocomposite for bone healing applications. *Mater. Sci. Eng. C* **2011**, *31*, 43–49. [CrossRef]
39. Sukyai, P.; Lam, N.T.; Niamsap, T. In situ biosynthesis of bacterial nanocellulose incorporated with hydroxyapatite/cellulose nanocrystals. *New Biotechnol.* **2018**, *44*, S11. [CrossRef]
40. Zhang, S.; Xiong, G.; He, F.; Huang, Y.; Wang, Y.; Wan, Y. Characterisation of Hydroxyapatite/Bacterial Cellulose Nanocomposites. *Polym. Polym. Compos.* **2009**, *17*, 353–358. [CrossRef]
41. Ahn, S.-J.; Shin, Y.M.; Kim, S.E.; Jeong, S.I.; Jeong, J.-O.; Park, J.-S.; Gwon, H.-J.; Seo, D.E.; Nho, Y.-C.; Kang, S.S.; et al. Characterization of hydroxyapatite-coated bacterial cellulose scaffold for bone tissue engineering. *Biotechnol. Bioprocess Eng.* **2015**, *20*, 948–955. [CrossRef]
42. Nudelman, F.; Pieterse, K.; George, A.; Bomans, P.H.H.; Friedrich, H.; Brylka, L.J.; Hilbers, P.A.J.; De With, G.; Sommerdijk, N.A.J.M. The role of collagen in bone apatite formation in the presence of hydroxyapatite nucleation inhibitors. *Nat. Mater.* **2010**, *9*, 1004–1009. [CrossRef]